River Research and Applications

WILEY

RESEARCH ARTICLE OPEN ACCESS

The Role of Sediment Supply on Fish Habitat Dynamics of a Morphologically Active River Widening

Mahmoud O. M. Awadallah[1] | Francesco Caponi[1] | David F. Vetsch[1] | Robert M. Boes[1] | Davide Vanzo[2]

[1]Laboratory of Hydraulics, Hydrology and Glaciology (VAW), ETH Zurich, Zurich, Switzerland | [2]Institute for Water and Environment, Karlsruhe Institute of Technology (KIT), Karlsruhe, Germany

Correspondence: Mahmoud O. M. Awadallah (awadallah@vaw.baug.ethz.ch)

Received: 10 December 2025 | **Revised:** 5 June 2026 | **Accepted:** 15 June 2026

Keywords: 2D hydrodynamic modeling | drought refugia | flood refugia | habitat complexity | hydro-morphology | resilient environment

ABSTRACT

Restoration measures, such as river widening, aim to reactivate key morphodynamic processes, which are critical drivers of fluvial habitat dynamics. While some evidence supports the important role of sediment supply on river widening's morphology, its link to fish habitat availability and dynamics remains unclear. To quantify this link, we used one-sided river widening morphologies formed under varying sediment supplies (100%, 80%, 60%, and 20% of the channel's transport capacity), upscaled from laboratory. The experiments started from a channelized alternating bar morphology that was subjected to a steady 1.5-year flood until equilibrium, followed by a 30-year flood event. We delineated the habitat for juvenile and adult brown trout (*Salmo trutta*) and evaluated their spatial dynamics across discharges, using 2-D hydrodynamic modeling and suitability curves. Our results showed that the near-equilibrium sediment supply morphologies (i.e., 100% and 80%) increased habitat at average to high flow conditions, with the 30-year flood further increasing low-flow habitats. In contrast, the widening morphologies formed with the reduced-sediment supply of 60% and 20% did not show an improvement in habitat quantities following both formative events. We found that the correspondence of the spatial habitat dynamics to morphodynamic processes depends on habitat location: juvenile habitats, typically occupying channel margins, corresponded to shoreline length dynamics, whereas adult habitats, typically found within the channels, corresponded to elevation change dynamics, both influenced by sediment supply. Our insights expand the understanding of sediment-habitat dynamics and can further assist holistic, resilient widening restoration strategies across multiple scales.

1 | Introduction

Fluvial morphodynamic processes are the main drivers of habitat dynamics. Through sediment deposition and erosion, habitat templates are continuously reshaped by morphological changes that modify the physical template of the riverbed (Poff et al. 1997; Wohl, Bledsoe, et al. 2015; Yarnell et al. 2015). The magnitude and the direction of these morphological changes are strongly controlled by the balance between sediment supply and transport capacity, with sediment deficit commonly promoting incision and sediment surplus favoring deposition (Lane et al. 1996; Kondolf 1997). These morphological adjustments cause spatial changes in the flow characteristics (e.g., flow depth and velocity) which influence aquatic species behavior, energy expenditure, food availability, and accessibility to essential habitats (Hauer et al. 2008; Sukhodolov et al. 2009; Wheaton et al. 2013; Tamminga and Eaton 2018; Farò and Wolter 2024; van Rooijen et al. 2024). While the

Davide Vanzo formerly at VAW-ETH Zurich.

dynamics of aquatic habitats in response to morphological changes have been increasingly studied, the quantitative link to the sediment supply underlying these morphological changes remains insufficiently understood.

Throughout history, anthropogenic interventions aimed at meeting human needs—flood control, water supply, hydroelectric energy, agriculture, urbanization, and navigation—have markedly altered the natural water and sediment regimes of river systems (Kondolf 1997; Wohl, Bledsoe, et al. 2015). These alterations have simplified river's habitat mosaics (e.g., by disconnecting the floodplains from their main channel) and increased the threats against hydromorphological, thermal, and other disturbances (Tonolla et al. 2010; McKean and Tonina 2013; Peipoch et al. 2015; Rachelly et al. 2021; Antonetti et al. 2023; Cashman et al. 2024). This has resulted in the degradation of many freshwater ecosystems, impairing their functionalities and resilience (Dudgeon et al. 2006; Hohensinner et al. 2011; Wohl 2024). Consequently, various restoration measures have been proposed to recover critical ecological functions in degraded river systems (Palmer et al. 2010; Wohl, Lane, and Wilcox 2015; Wohl 2024). These measures commonly aim to restore natural hydrological flow, sediment, and wood regimes to regain geomorphic complexity, provide more space for rivers, and enable crucial processes (Poff et al. 1997; Gurnell et al. 2002; Rohde et al. 2005; Wohl, Bledsoe, et al. 2015; Yarnell et al. 2015; McCabe et al. 2025).

Sediment starvation (i.e., sediment availability below the transport capacity) is a known issue in regulated gravel-bed rivers, where damming, bed load traps, gravel extraction, and channelization can reduce sediment availability and/or increase transport capacity, ultimately promoting channel deepening and incision (Kondolf 1997; Rollet et al. 2014). Different countermeasures can target the recovery or restoration of sediment regimes, such as self-forming, dynamic river widenings and gravel augmentation, to reactivate essential morphodynamic processes (Rohde et al. 2005; Wohl, Bledsoe, et al. 2015; Pauli et al. 2018). Dynamic river widening, by removing bank protections to allow lateral erosion and channel shifting, helps reconnecting rivers with their floodplains and enhances habitat heterogeneity (Rachelly et al. 2022). Although sediment supply has been shown to influence the morphological trajectory of river, how this translates into aquatic habitat availability and dynamics remains unclear (Reid et al. 2020; Rachelly et al. 2022; Soto Parra et al. 2024).

The interrelation between sediment regime/availability and aquatic habitat dynamics has been increasingly highlighted in recent fluvial geomorphology studies. For example, sediment supply has been found to actively influence salmonid habitats, leading to a non-stationary habitat-discharge relationship as found by Reid et al. (2020). Soto Parra et al. (2024) investigated fish habitat dynamics for brown trout in two consecutive alpine reaches subjected to the same flood event but different sediment regimes, and found that the reach with higher sediment supply showed greater habitat dynamics than the starved-sediment reach. Yet, a quantitative link to the sediment supply condition that caused these habitat dynamics is still missing. This arises from the difficulties: (i) associated with the direct measurements that enable quantification of the sediment being supplied (Soto Parra et al. 2024; Wohl 2024) and (ii) in isolating the effect of sediment supply and flood characteristics on the habitat dynamics using a before-after approach in real river sites (Wohl 2024).

This work aimed at quantifying the effect of sediment regime on aquatic habitat availability and dynamics at different flow conditions, ranging from droughts to floods. Using 2D hydrodynamic modeling and habitat suitability curves, we disentangled the effect of sediment regime on fish habitat dynamics by exploiting a dataset of digital elevation models derived from a series of laboratory experiment of a one-sided river widening, formed under different sediment supplies and flood events (Rachelly 2021; Rachelly et al. 2022). We used juvenile and adult brown trout fish as proxies for aquatic habitats. We further investigated the underlying morphodynamic processes associated with habitat stability and change (i.e., hereafter referred to as spatial habitat dynamics) and their variabilities with sediment supply. We linked these dynamics to morphological metrics, namely shoreline length (Ward et al. 1999) and elevation changes. The used dataset from the experimental setting allows the effect of sediment supply on fish habitat dynamics to be isolated from other confounding processes (e.g., vegetation, macroroughness, wood load) (Montgomery and Piégay 2003; Bertoldi et al. 2014). Our study tries to address the following research questions:

1. How does sediment supply, and the resulting morphological changes, influence brown trout's habitat availability and dynamics under different flow conditions?
2. What is the influence of a moderate flood event (30-years flood) on habitat availability and dynamics, and how does this vary with sediment supply?
3. What morphological processes drive the spatial habitat dynamics, and how does the sediment supply influence them?

2 | Data and Methods

2.1 | Reference Reach and Experimental Morphology Datasets

2.1.1 | Reference Reach

The morphologies used in this study originate from laboratory experiments by Rachelly (2021). The aim of the experiment was to assess the morphodynamic response of a channelized reach, subjected to different sediment supply conditions, to a one-sided dynamic river widening. The experimental channel was designed to resemble a reach at the Kander River, Switzerland, an originally wandering subalpine gravel-bed river. The reach has a channel width ranging from 20 to 25 m, a longitudinal slope of 1%, and poorly sorted sediments of 6 cm mean diameter (Rachelly et al. 2021). In the period between 1980 and 2021, the reach experienced a mean annual discharge (Q_m) of about 20 m^3/s, highest flow of 270 m^3/s (~13.5 Q_m), equivalent to a 60-year flood, and minimum flow of 3 m^3/s (~0.15 Q_m) (Figure A1a). With respect to dominant fish species, the reach can be considered as a transitional

fish region of lower trout (*Salmo trutta*) and upper grayling (*Thymallus thymallus*) (Huet 1949).

2.1.2 | Laboratory Widening Experiments

The physical experiment at prototype scale (Froude scale factor $\lambda = 30$) had an initial trapezoidal channel with a bottom width of 26.8 m and 2:3 (v:h) bank slopes over a length of 897 m (light gray section in Figure 1a). On the right bank side, the width of the channel was allowed to freely widen up to 107 m in total (i.e., widening ratio of 4) over a length of 708 m (dark gray section in Figure 1a). The widening floodplain had an initial vertical offset of 2.1 m which is equivalent to the water surface elevation of a 30-years flood in the reference reach. The widening process from an initial channelized alternating bar morphology (hereafter termed as "channelized", T_0) was dynamically initiated by two consecutive hydraulic conditions (Rachelly 2021) (Figure 1b): (i) a steady bed-forming discharge of 1.5-years flood ($HQ1.5 = 118.3\,m^3/s$ in prototype), representing long-term exposure to a bed-forming discharge, followed by (ii) a hydrograph event with a peak flow of 30-year flood ($HQ30 = 244\,m^3/s$ in prototype). For the steady HQ1.5 flood phase, the experiments were continued until a transport equilibrium had been established and no more significant morphological changes observed. The hydrograph shape and duration of the HQ30 flood was designed to roughly correspond to such an event at the reference reach. These widening evolutions were produced under different sediment supply levels (SSL): 100%, 80%, 60%, and 20% of the trapezoidal channel's transport capacity (TC). The sediment was supplied to the flume inlet using a sediment feeder with an accuracy of ±0.5%. This sediment was identical to the sediment of the mobile bed of the channel and floodplain. More details on the experimental setup, methodology, and program can be found in Rachelly et al. (2022).

2.1.3 | Digital Elevation Models Used in This Study

In this study, we referred to the initial channelized alternating bar as the "channelized" state (T_0), the state after the steady bed-forming of HQ1.5 as "widening" (T_1), and the one after the HQ30 event as "after HQ30" (T_2). We focused on a total of 12 topographical scans (in the form of digital elevation models, DEM, 0.3×0.3 m in prototype) (Figure 1b): Three different temporal snapshots of the widening evolution (i.e., channelized, widening, and after HQ30) for each of the four SSLs (100%, 80%, 60%, and 20% of TC). We defined two morphological evolution phases for the widening (hereafter termed as morphological phases; Figure 1b): (i) the "formation phase" (T_1–T_0), that is, from channelized to widening, and (ii) the "HQ30 flood phase" (T_2–T_0), that is, from channelized to after HQ30.

2.2 | Hydrodynamic Numerical Model

To obtain water depth and flow velocity, 2-D hydrodynamic modular freeware BASEMENT v4.0.2 (Vetsch et al. 2023) was used, which solves the 2-D shallow water equations with a finite volume method on unstructured computational meshes (Vanzo et al. 2021). We used a calibrated model provided by the study of Rachelly et al. (2021) and re-ran it for a discharge range considered in this study. The computational meshes were generated using the QGIS plugin BASEmesh v2 (Vanzo et al. 2021). The number of cell elements was 107,234 elements for the channelized state models and increased to 248,944 elements for the widening and after HQ30 states models. For all, the elements area

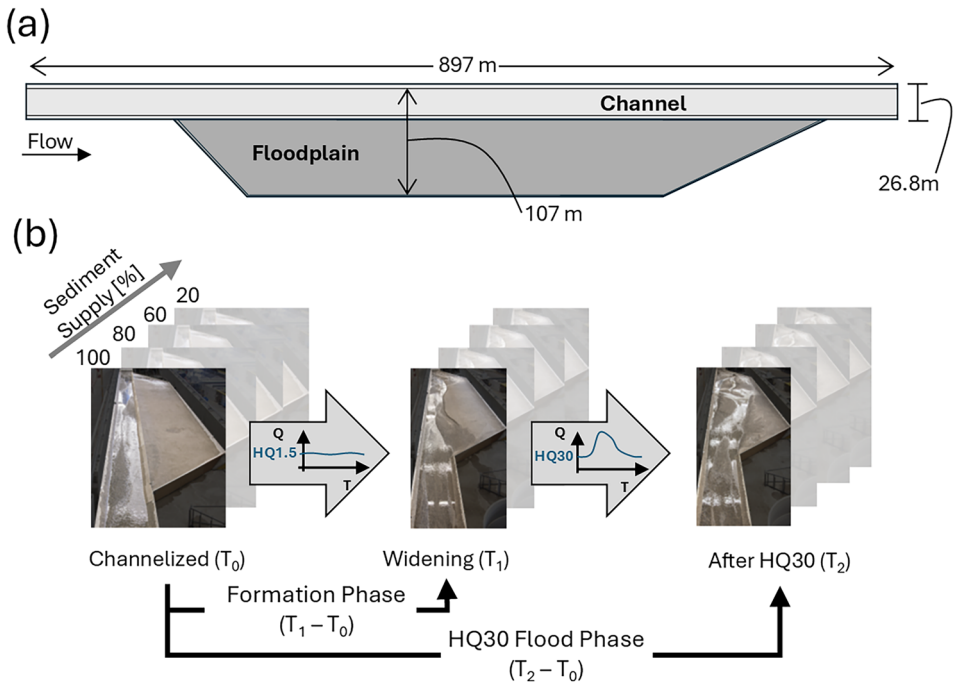

FIGURE 1 | (a) Plan view layout for the one-sided widening setup in prototype scale. The light gray indicates the initial channel section and the dark gray section indicates the available floodplain for widening. (b) Experimental program used for the widening development with different sediment supply levels (adapted from Rachelly (2021)). [Color figure can be viewed at wileyonlinelibrary.com]

ranged between 0.09 m^2 to 0.5 m^2 with an average size of 0.3 m^2. The calibration resulted in a uniform Strickler roughness coefficient of 30 $m^{1/3}/s$ which was kept fixed for all hydrodynamic simulations. Uniform flow conditions were applied at the upstream and downstream boundaries by imposing constant inflow discharge at the upstream boundary condition and uniform flow depth at the downstream boundary condition. The minimum water depth to distinguish between wet and dry cells was set to 0.01 m. The simulated discharges were ranging between 2.5 m^3/s (0.125 Q_m≈historical minimum) to 120 m^3/s (6.0 Q_m≈ HQ2) with 2.5 m^3/s increment (i.e., 47 simulated discharges in total) as the focus was on flow conditions ranging from drought to small flooding conditions.

2.3 | Fish Habitat Modeling

Brown trout (*Salmo trutta*) at the two life stages juvenile (JBT) and adult (ABT) were selected as proxies for fish species at the reference reach. The extents of the suitable areas were delineated using empirically derived hydraulic suitability curves from literature for the two life stages (i.e., for JBT after Hauer et al. (2014) and for ABT after Heggenes (1996); Figure 2). We used the water depth and velocity suitability indices for the estimation of the overall suitability. Because 2D substrate maps were not available from the experimental lab dataset, the substrate suitability index was excluded from the overall habitat suitability estimation, despite the known importance of substrate for

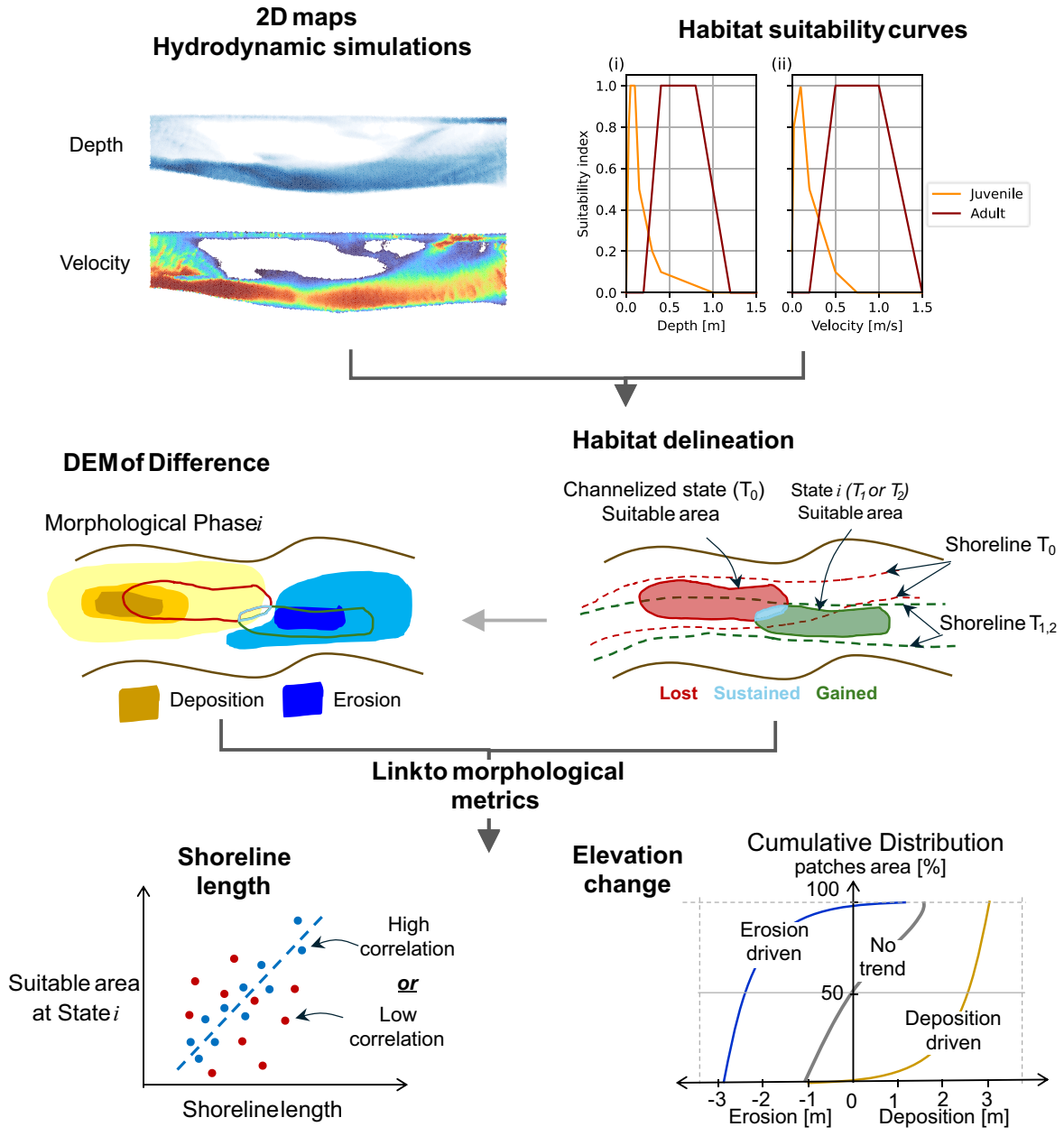

FIGURE 2 | Workflow diagram for the steps of habitat dynamics evaluation and the link to morphological metrics (i.e., shoreline length and elevation changes). The overall habitat suitability (HSI ≥ 0.5) based on depth and velocity was estimated for juvenile brown trout after Hauer et al. (2014) and for adult brown trout after Heggenes (1996). The possible interpretations of the habitat dynamics relationship to the two morphological metrics are presented. [Color figure can be viewed at wileyonlinelibrary.com]

brown trout habitat suitability, particularly during spawning (Heggenes 1996). However, it should be noted that the grain size distribution of the fed sediment remained unchanged, meaning that no external source of sediment fining or coarsening was introduced. The overall habitat suitability (HSI) was computed as the geometric mean of water depth and flow velocity suitabilities for each computational cell (e.g., Wakeley 1988; Boavida et al. 2014; Tamminga et al. 2015). The total suitable area was calculated by adding up the area of all cells with HSI ≥ 0.5 (e.g., Moniz and Pasternack 2021; Antonetti et al. 2023). A sensitivity test of this threshold was carried with increasing and lowering this threshold by 50%. The total suitable area was then normalized with respect to the full computation domain (i.e., similar to the wetted area) and referred to as the "normalized suitable area".

2.4 | Evaluation of Habitat Dynamics

2.4.1 | Wetted Areas and Hydraulic Variables Distributions

The resulting wetted area at any discharge scenario was computed as the sum of the wetted cells (i.e., with minimum water depth of 0.1 m) and normalized by the full computation domain (A_{tot} = channel + widening = 77,064 m^2; Figure 1a). In addition, we obtained the water depth and velocity distributions based on the computational cells and compared them across morphological states and SSLs.

2.4.2 | Suitable Habitat-Discharge Relationship

The total suitable area for the JBT and ABT was calculated at any discharge, morphological states (i.e., channelized, widening, and after HQ30), and SSLs. Depending on the location, the suitable areas were classified into: (i) channel habitat, the sum of area located within the initial channelized section (light gray area in Figure 1a); and (ii) floodplain habitat, the sum of area located in the newly available widened area (dark gray area in Figure 1a). This classification allowed to detect where the suitable habitat increase, decrease, or remained unchanged following the widening evolution. Moreover, we used the discharge duration curve, calculated from the reference flow series between 1981 and 2021 (Figure A1a), to estimate the habitat duration curve (Capra et al. 1995).

2.4.3 | Spatial Habitat Dynamics Evaluation

To analyze the spatial habitat dynamics following a morphological phase, three habitat states were defined (Figure 2): (i) *lost*, where suitable areas from the channelized state became unsuitable in the subsequent states; (ii) *gained*, where new suitable area appeared (i.e., previously unsuitable areas) in the following state; and (iii) *sustained*, where suitable areas persisted as suitable in the following state. A similar approach for investigating the habitat dynamics was also used by Moniz and Pasternack (2021). We focused the evaluation on three representative discharges (Figure A1b): (i) 0.25 Q_m, representing conditions at low flows (mimicking drought conditions; typically exceeded almost ~100% of the year), (ii) 2.0 Q_m, representing average to decently above average flow conditions (exceeded around 10% of the year), and (iii) 4.0 Q_m, representing annual high flow conditions (exceeded only 0.5% of the year).

2.4.4 | Links to Morphological Metrics

The link of the spatial habitat dynamics to the driving morphodynamic processes was attempted using: (i) the shoreline length (km/km), which measures the complexity (i.e., perimeter) of the wetted area and marginal zones (Ward et al. 1999), and (ii) the elevation changes following a morphological phase. For the shoreline length, 2 km/km reflects a shoreline length of a flat-bed straight channel and higher indicates more complex wet boundaries. We tested whether the increase or decrease of the suitable area for a given scenario corresponds to a change in the respective shoreline length. The elevation changes (m) following a morphological phase (Figure 1b) was quantified using DEM of difference (DoD). The mean elevation changes within the lost, gained, or sustained habitat polygons were estimated using the zonal statistics tool in QGIS (Figure 2). A propagated error of the resulting DoD of 0.085 m (Rachelly et al. 2021) was considered for the true elevation changes with a Student's *t*-test and a confidence level of 95% (Wheaton, Brasington, Darby, Merz, et al. 2010). The results were then presented in cumulative frequency distributions curves (Figure 2). Depending on the curve's shape, the lost, gained, or sustained suitable habitat could: (i) be deposition driven, if the elevation change within the polygon is mostly at depositional change; (ii) be erosion driven, if the elevation change within the polygon is mostly at erosional change; (iii) have no trend, if the change is distributed across all elevation changes. This analysis was also conducted for the three representative discharges (i.e., 0.25, 2.0, and 4.0 Q_m). It is worth mentioning that, when comparing the habitat dynamics with the morphological changes resulting from the HQ30 flood phase, using either shoreline length or elevation change, the comparison also includes the effect of the preceding formation phase (Figure 1b). Therefore, the interpretation of the habitat dynamics and their link to the morphological metrics should acknowledge that the effect of the HQ30 flood phase cannot be fully isolated.

3 | Results

3.1 | Wetted Areas and Hydraulics

The variability of the wetted areas with discharge for the three morphological states (i.e., channelized, widening, and after HQ30 states) is shown in Figure 3a. Before the widening started, all SSL scenarios displayed similar wetted area ranges, increasing from 0.18 A_{tot} to 0.30 A_{tot} (~70% increase) at 2.0 Q_m (bars became fully submerged) and showed only a marginal increase at higher discharges.

After the formation phase, the early activation of the widening at around "1–2 Q_m" for 100% and 80% SSL allowed a rapid increase in inundation, reaching ~0.9 A_{tot} by 4.0 Q_m (~300% increase from the channelized state). The greater morphological activity at these scenarios resulted in the formation

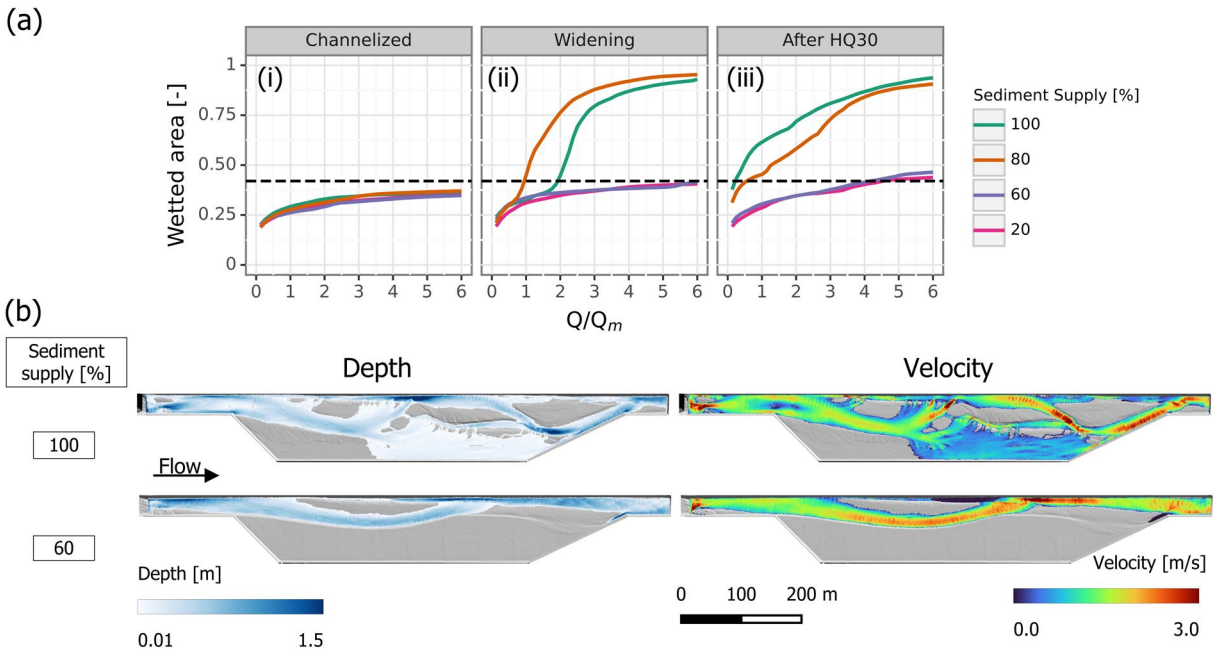

FIGURE 3 | (a) Wetted area variation with discharge at the three morphological states for all sediment supply levels: Channelized (i), widening (ii), and after HQ30 (iii); (b) spatial distribution of water depth and flow velocity at mean discharge ($Q_m = 20\,m^3/s$) at the after HQ30 state for 100% and 60% sediment supply scenarios (top view). The wetted area is normalized by the total model area (A_{tot}). The horizontal dashed line represents the area of the channelized part (i.e., the channel in Figure 1a). [Color figure can be viewed at wileyonlinelibrary.com]

of central and side bars that led to heterogeneous flow fields and enhanced channel-floodplain connectivity (Rachelly et al. 2022). This resulted in higher hydraulic variability with wider water depth and flow velocity ranges across average to high discharges (Figures A2 and A3). In contrast, the 60% and 20% SSL exhibited limited increases in inundations due to the inactive widening, with maximum wetted area of 0.4 A_{tot} at highest discharge (6.0 Q_m), which is still below the maximum channel area ($A_{ch} = 0.42\ A_{tot}$). Following the HQ30 event, the 100% SSL scenario consistently exhibited the highest wetted area across all discharges, surpassing the 80% SSL scenario (Figure 3a). At low discharges (< 0.5 Q_m), wetted areas for both 100% and 80% SSL increased by over 100% compared to the widening state. On the other hand, the 60% and 20% SSL scenarios showed almost no changes following the HQ30 flood phase, apart from a minimal increase at discharges higher than 4.0 Q_m (Figure 3b).

3.2 | Suitable Habitat Variation With Discharge

Figures 4 and 5 illustrate the variation in suitable area with discharge for JBT and ABT, classified as in the channel (Figure 4a,d,g for JBT; Figure 5a,d,g for ABT), floodplain (Figure 4b,e,h for JBT; Figure 5b,e,h for ABT), and total (Figure 4c,f,i for JBT; Figure 5c,f,i for ABT).

For JBT, the channel habitats maintained the same shape and range for all SSL scenarios (Figure 4a,d,g). The habitat area peaked at low discharges (~0.01 A_{tot} at 0.125 Q_m) and steadily decreased with discharge increase to nearly vanishing at high flows. On the other hand, the floodplain habitat for the 100% and 80% SSL scenarios increased significantly in the widening state (Figure 4e) at discharges activating the widening (Figure 3a), peaking to ~0.10 A_{tot} at "1–2 Q_m" before declining to ~0.01 A_{tot} at 4.0 Q_m. The HQ30 flood event further reduced the peak floodplain habitat, and thus the overall suitable areas, to ~0.04 A_{tot} (a 60% reduction) but increased suitable areas at low discharges (< 1 Q_m) (Figure 4g–i). For the 60% and 20% SSLs, almost no floodplain habitat existed as the widening remained inactive after the two morphological phases (Figure 3a). Finally, the overall suitable areas for the JBT showed to be sensitive to the threshold of the overall habitat suitability (Figure A4), but without changing the trends observed for the different SSL scenarios.

For ABT, in general, the habitat quantities were consistently larger than JBT habitats by about one order of magnitude (Figure 5). Similar to JBT, the formation and HQ30 flood phases slightly increased total suitable areas for the 20% and 60% SSLs by increasing the suitable areas in the channel at low flows (< 1 Q_m) and in the floodplain at high flows (> 4 Q_m). For the 100% and 80% SSLs, however, floodplain habitat increased significantly at discharges corresponding to floodplain activation (1 to 2 Q_m) reaching ~0.5 A_{tot} and remaining at that level up to 6.0 Q_m, while channel habitats showed only marginal increases (Figure 5d). The HQ30 flood event reduced the maximum floodplain habitat to ~0.3 A_{tot} (Figure 5h) while increasing both channel and floodplain habitats at low flows and maintaining this level consistently across all discharges (0.125 to 6.0 Q_m). Finally, unlike JBT, ABT overall suitable areas showed little sensitivity to changes in the threshold used to define overall habitat suitability (Figure A4).

The habitat duration curves for the morphological states of the 100% and 20% SSL are shown in Figure A5. For the JBT (Figure A5a), the 20% SSL maintained 0.01 A_{tot} habitat area across most of annual conditions at all states. This was also the

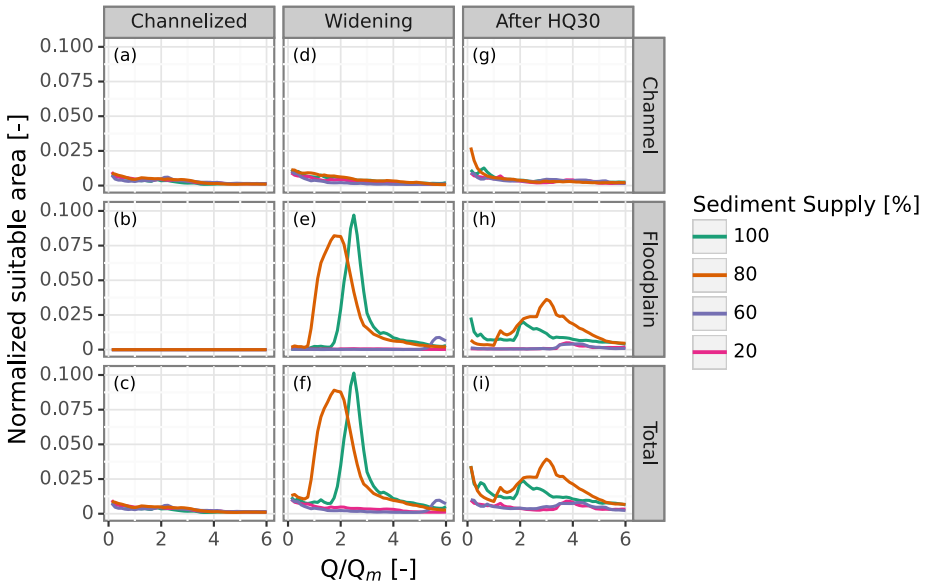

FIGURE 4 | Normalized suitable area variation with discharge for juvenile brown trout (JBT) at the different morphological states: Channelized (a–c), widening (d–f), and after HQ30 (g–i), separated as areas located in channel (a, d, and g), floodplain (b, e, and h), and in total (c, f, and i). [Color figure can be viewed at wileyonlinelibrary.com]

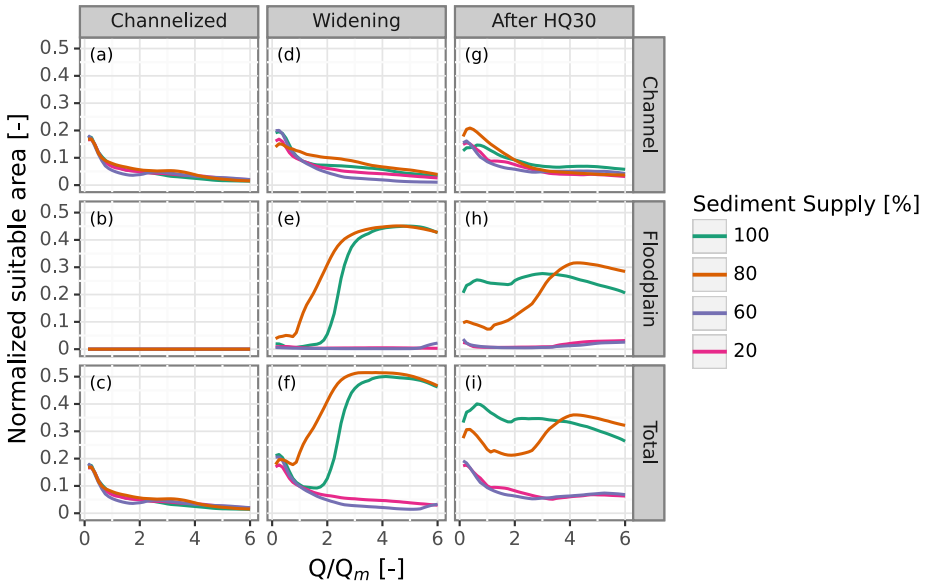

FIGURE 5 | Normalized suitable area variation with discharge for adult brown trout (ABT) at the different morphological states: Channelized (a–c), widening (d–f), and after HQ30 (g–i), separated as areas located in channel (a, d, and g), floodplain (b, e, and h), and in total (c, f, and i). [Color figure can be viewed at wileyonlinelibrary.com]

case for around 85% of the yearly conditions (approximately 62 days out of 365) for the 100% SSL after the formation phase. Following the HQ30 flood, the available habitat area throughout the year increased by 100% (from 0.01 to 0.02 A_{tot}) for the 100% SSL scenario. For the ABT (Figure A5b), the formation and HQ30 flood phases for the 20% SSL consistently increased habitats by an area of 0.02 to 0.04 A_{tot} annually compared to the channelized state. For the 100% SSL, the formation phase increased the habitat area by an area of 0.05 A_{tot} for 85% of the year (around 300 out of 365 days), with a significant increase in periods of discharges >2.0 Q_m (~15% of the yearly flow). The available suitable areas for most of the yearly conditions (~95% of the year) after the HQ30 flood increased by 200% to 300% compared to after the formation phase.

3.3 | Spatial Habitat Dynamics With Discharge

For JBT, no sustained habitats from the channelized state were observed across all discharge conditions (Figure 6a,b). Following the formation phase, gained and lost habitats at low flow conditions were almost equal for all SSL scenarios. This

trend continued also at higher discharges for the 60% and 20% SSLs. For the 100% and 80% SSL scenarios, however, the gained greatly surpassed the lost habitats.

For ABT (Figure 6c,d), the sustained habitat from the channelized state comprised about 40% of the total habitats at low flows for the 100% and 80% SSL scenarios after the formation phase (Figure 6c) and about 60% of the 60% and 20% SSL habitats. After HQ30, this portion remained the same for the 60% and 20% SSL while significantly decreasing for the 100% and 80% SSLs, as the gained habitat greatly increased. As the discharge increases, sustained habitat decreases across all SSL scenarios; however, it remained a considerable portion (more than 20%) of the total habitat for the 60% and 20% SSLs. The lost and gained areas for the 60% and 20% SSLs were consistently in the same order of magnitude throughout discharge conditions, which was not the case for the 100% and 80% SSLs.

3.4 | Spatial Habitat Dynamics and Morphodynamic Processes

The spatial distributions of the elevation changes following the formation phase for the 100% and 20% SSLs and the locations of the lost, gained, and sustained patches at low and high flow conditions for JBT are shown in Figure 7. For all, the individual JBT habitat patches were relatively small in area (Mean ± SD; $0.9 \pm 0.5\,m^2$) and primarily located along the boundaries of the wetted channels (Figure 7c–f). The habitat states for the same scenarios for ABT are shown in Figure 8. Compared to the JBT habitat, the individual patch area of the ABT habitat was larger (Mean ± SD; $26.1 \pm 23.9\,m^2$) and primarily located at the center of the wetted channels (Figure 8).

With respect to elevation changes, no trends were observed to favor any particular habitat status for the JBT at any of the

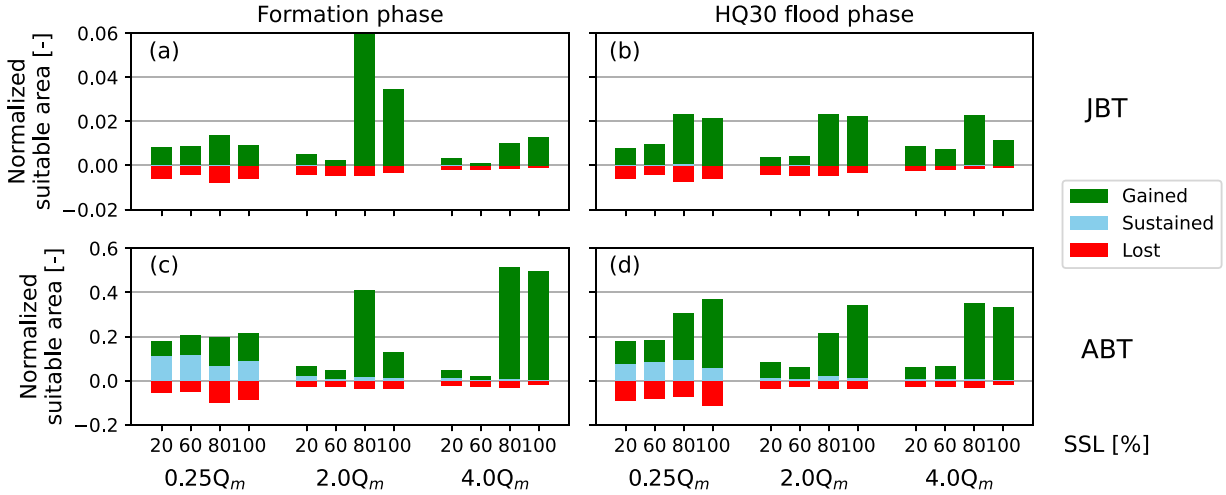

FIGURE 6 | Normalized suitable area changes (i.e., lost or gained) and stability (i.e., sustained) from the channelized state for selected discharges (i.e., 0.25, 2.0, and 4.0 Q_m) for juvenile brown trout (JBT) (a, b) and adult brown trout (ABT) (c, d) and different sediment supply levels (SSLs). The lost suitable areas were plotted on the negative side of the *y*-axis. [Color figure can be viewed at wileyonlinelibrary.com]

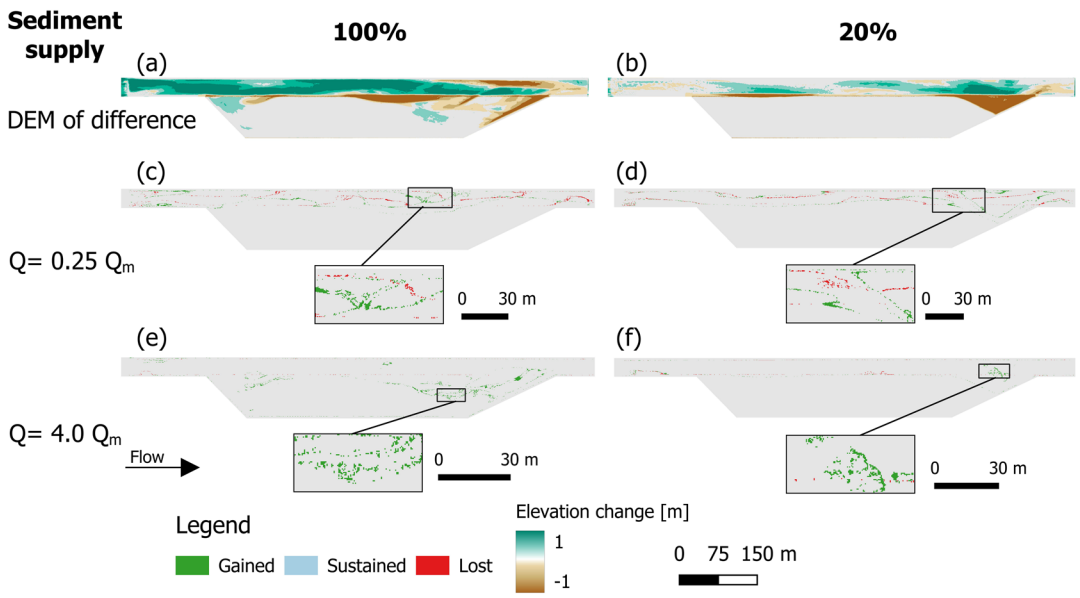

FIGURE 7 | Spatial distribution of elevation changes (a, b) following the formation phase for the 100% and 20% sediment supplies, and lost, gained, and sustained patches at low (c, d) and high (e, f) discharges for juvenile brown trout (JBT). [Color figure can be viewed at wileyonlinelibrary.com]

discharge conditions (as also demonstrated by the cumulative distributions plots; Figures A6–A8 for JBT). With respect to shoreline length, the correlation between the suitable area (at all morphological states) and the length of the shoreline showed to be very high ($R^2 > 0.9$) for all SSL scenarios (Figure 9). As reported by Rachelly et al. (2021), the shoreline length for the widening states at the 100% and 80% SSL scenarios increased at discharges activating the widening region (Figure A9). At higher discharges, where the inundation boundaries reach the boundary of the model (i.e., equivalent in prototype to the restoration area perimeter), the shoreline length drops. The shape of the JBT suitable area relationship with discharge (Figure 4c,f,i) showed to resemble the shoreline length-discharge pattern for the different SSLs (Figure A9).

For ABT, the correlation between the suitable habitat area and the shoreline length was weaker ($R^2 < 0.5$; Figure A10). With respect to elevation change, however, the correspondence was clearer (Figure 10). At low flow conditions (Figure 10a–f), over 90% of the lost areas was at depositional change locations in both SSL scenarios, with the 100% SSL being at higher depositional changes (Figures 8c,d and 10a). This trend was not affected by the HQ30 flood event (Figure 10d). The gained patches were distributed between both elevation change (i.e., deposition and erosion) for the 100% SSL (Figure 8c) with no specific trend (Figure 10b). For the 20% SSL, however, the gained patches were observed to favor erosional change's locations (~50%) while the remaining fluctuated between no to minor depositional changes (Figure 10b). The HQ30 flood shifted the gained patches to locate in erosional areas for both SSL scenarios (Figure 10e), with the gained patches at the 20% SSL showed to correspond to higher erosions (more than 50% at higher than 1 m erosion). The sustained patches at the 20% SSL were observed to be located at minor deposition to no elevation change (Figures 8d and 10c). After the HQ30 flood, the sustained habitats showed to locate at erosional changes mainly (Figure 10f). For the 100%

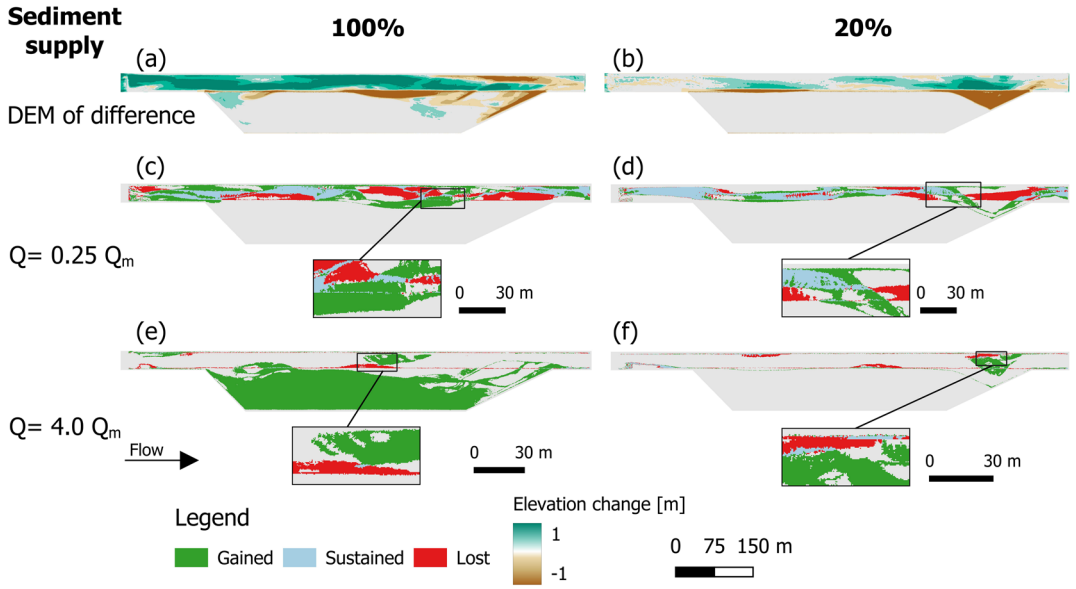

FIGURE 8 | Spatial distribution of elevation changes (a, b) following the formation phase for the 100% and 20% sediment supply scenarios, and lost, gained, and sustained patches at low (c, d) and high (e, f) discharges for adult brown trout (ABT). [Color figure can be viewed at wileyonlinelibrary.com]

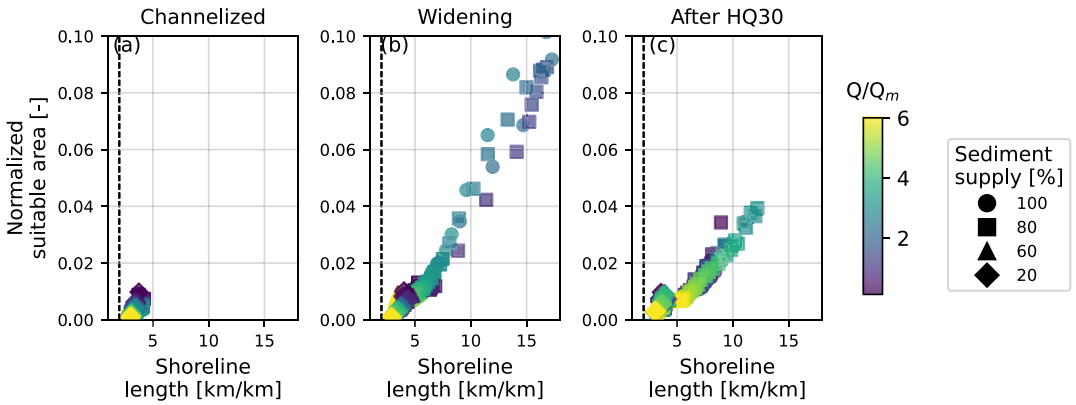

FIGURE 9 | Shoreline length relationship with juvenile brown trout suitable area for the different morphological states: (a) channelized; (b) widening; and (c) after HQ30. The vertical dashed line indicates a shoreline length of 2 km/km, corresponding to a straight flat-bed channel. [Color figure can be viewed at wileyonlinelibrary.com]

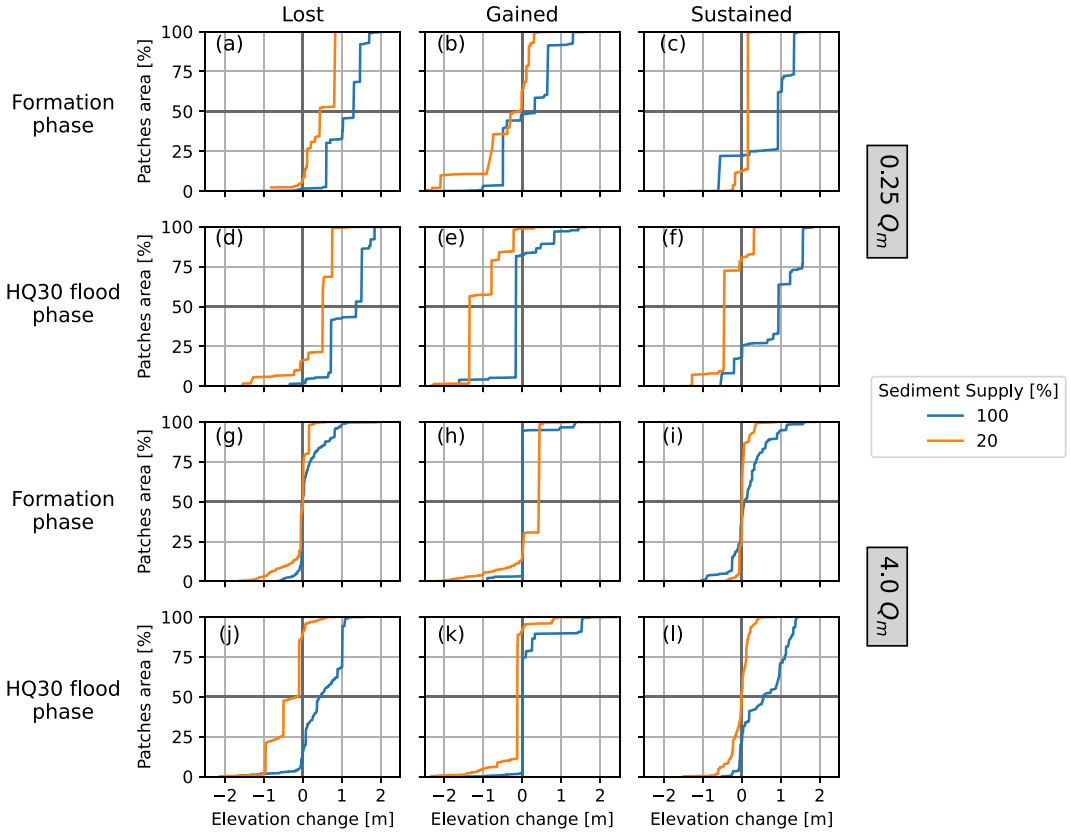

FIGURE 10 | Cumulative distribution of mean elevation changes within adult brown trout habitat patches classified as lost (a, d, g, j), gained (b, e, h, k), and sustained (c, f, i, l). Results are shown for the low-flow scenario (0.25 Q_m; a–f) and high-flow scenario (4.0 Q_m; g–l), during the formation phase (a–c and g–i) and the HQ30 flood phase (d–f and j–l), for the 100% and 20% sediment supply scenarios. [Color figure can be viewed at wileyonlinelibrary.com]

SSL scenario, the sustained patches showed to be located at depositional changes, regardless of the phase (Figure 10c,f). At high flow conditions (Figures 8e,f and 10g–l), lost patches for both SSL scenarios were mostly in areas with no elevation change (~75% of the area), with the remaining at depositional areas for the 100% SSL and at erosional areas for the 20% SSL (Figure 10g). The HQ30 flood increased the correspondence of the latter elevation changes and reduced the no elevation change correspondence (Figure 10j). The gained patches, on the other hand, appeared to be located at no elevation change for the 100% SSL (more than 90% of area; Figure 10h), while for the 20% SSL was mainly at depositional changes (~70%). The HQ30 flood shifted the gained patches of the 20% SSL to locations with no elevation change, while the 100% SSL trend remained the same (Figure 10k). Although the sustained habitats at high flow conditions were very small (Figure 8e,f), the trend of the low flow conditions was relatively preserved (i.e., at depositional and no changes for the 100% and 20% SSLs, respectively) (Figure 10i,l).

4 | Discussion

4.1 | Habitat Dynamics Across Sediment and Hydrologic Conditions

Channel-floodplain connectivity and overbank accessibility are crucial for maintaining diverse fish habitats. These connections facilitate fish mobility between the river and floodplain, providing access to essential habitats for different life stages, including spawning, foraging, and refuge during high flows (Sullivan and Watzin 2009; Bolland et al. 2012; Bouloy et al. 2024). In this study, we found that the reduced sediment supply scenarios (i.e., 60% and 20% SSL) did not enhance the channel-floodplain connectivity, as was observed at the near-equilibrium sediment supply scenarios (i.e., 100% and 80% SSL), resulting in limiting the habitat availability of brown trout (Figures 4 and 5). The limited reworked morphologies observed at the reduced-sediment supply scenarios led to morphologies not different from the initial channelized state (Figure 3b), preserving the habitat-discharge relationship of that state (Figures 4 and 5). At low to average discharges, the alternating bar morphologies (i.e., channelized state) are able to provide some degree of hydraulic variability and habitat heterogeneity compared to flat-bed morphology (e.g., Hauer et al. 2014; Vanzo et al. 2016). The discharge increase in these confined morphologies expands fast-run habitats domination and reduces slower-flow areas that preferred by brown trout (Hauer et al. 2014; Mandlburger et al. 2015; Reid et al. 2020). The effect of reduced-sediment scenarios on discharge–habitat relationship was also noted by Mortensen et al. (2024), who found that the channel deepening and floodplain disconnection, occurred at post-dam morphology, limited the increase of shallow and low-velocity habitats to be present only at higher discharges. This was also observed in our results. The reduced-sediment scenarios showed to intensify the hydraulic conditions, with depth and velocity distributions

shifted toward higher values and narrower ranges already at average flow conditions (Figures A2 and A3). Because the habitat model is driven by depth and velocity suitability, this shift indicates that the reduced-sediment morphologies provide fewer slow and shallow hydraulic conditions suitable for brown trout, particularly for juveniles. This highlights that even the yearly average flow condition might form a hydraulic bottleneck for brown trout, potentially leading to downstream drifts of juveniles (Hauer et al. 2014). The near-equilibrium sediment supply scenarios, through the connected channel-floodplain morphologies, showed greater habitat availability for brown trout at broader discharge conditions, especially at high flow conditions (Figures 4 and 5). This supports that river ecosystems with near-natural sediment regimes are likely to promote resilient environment that are capable to provide necessary ecological functions at various hydrological conditions (Poff et al. 1997; Wohl, Bledsoe, et al. 2015; Benjankar et al. 2025).

4.2 | Flood-Driven Temporal Evolution of Habitats

Flood events are able to shape the fluvial habitats by reshaping the channel and floodplain landforms (Wohl, Bledsoe, et al. 2015; Yarnell et al. 2015). Depending on sediment availability, the impact of flood events on the dynamics of habitat varies (Soto Parra et al. 2024). In our setting, the HQ30 event at the near-equilibrium scenarios triggered hydromorphological activity that resulted in substantial reworked morphologies, as reported by Rachelly et al. (2022). We found that this reworking increased the habitat availability at flow conditions more frequently exhibited in the reach (Figure 5A) and decreased the availability at high-flow conditions for both life stages (Figures 4 and 5). However, this response should not be interpreted as a general effect of HQ30 floods, as the increase in low-flow habitat is likely linked to the initial widening configuration (e.g., the floodplain elevation offset, the experimental geometry, and the morphology state before the HQ30 event) which controlled the extent of floodplain reworking and reconnection. Aramburú-Paucar et al. (2024) investigated the response of a regulated reach at the lower Serpis River (Spain), where tributaries and steep hillslopes provide sediment inputs to the reach, to an 18-year flood event. They showed that the flood increased the morphological complexity and hydraulic heterogeneity, compared to pre-flood state, resulting in an increase in habitat at low flow conditions. The reduction in habitats at high-flow conditions was also shown by Moniz and Pasternack (2021) where overbank rearing habitat for Chinook salmon (*Oncorhynchus tshawytscha*) decreased following series of flood events of 3–5-year return periods. On the other hand, we found that the HQ30 flood at the reduced-sediment supply scenarios resulted in only marginal hydromorphological changes, with limited improvements in habitat availability (small increase in ABT habitat at $>4.0\ Q_m$; Figure 5). Soto Parra et al. (2024) have documented similar distinctive morphological responses of two contiguous reaches subjected to a 1-year flood event but different sediment availability (due to an active sediment supply tributary). They also concluded that in the starved-sediment reach (which could correspond to the 60% and 20% SSL scenarios in our study), longer timescales or multiple high-flow events may be required for the morphology to move from the stable single-threaded conditions to a more dynamic (i.e., multi-threaded) state and achieve a clearer habitat replenishment. While the positive role of flood events in habitat restoration is widely recognized (Robinson et al. 2003; Hayes et al. 2018; Talbot et al. 2018; Doering et al. 2021), our findings underscore the key role of the associated sediment regime in determining the effectiveness of habitat replenishment. Without sufficient sediment, widening restoration and high floods may fail to achieve meaningful ecological improvements in regulated streams.

4.3 | Sediment Supply Effect on Morphodynamic Processes Driving Fish Habitat Dynamics

Our study highlights that fish habitat dynamics is often triggered by dynamics of the morphological features preferred by the life stage. Channel margins and shallow areas are known to offer important habitat for fish species in their juvenile stages (Hauer et al. 2014). In a dynamic morphology, these morphological features are susceptible to shift and change, even under small disturbances (Figure 7). The high potential of spatial relocation in these features reduces the opportunity of the habitat to locally persists post to a disturbance event (Figure 6a,b). On the other hand, adult habitats are primarily associated with more stable morphological features, such as pools, that are resilient to small morphological changes (Figure 8). Therefore, the habitat dynamics for the JBT habitats showed to be driven by changes in the margins' extent and location (Figures 7 and 9), regardless of the morphological disturbance (i.e., elevation change) associated with these dynamics (Figures A6–A8). Accordingly, the lost JBT habitats mainly represent localized patches along the shoreline of the Channelized state that were no longer suitable at the same locations after morphological changes. On the contrary, to induce habitat dynamics for the ABT, a meaningful morphological change is needed to mobilize these features (Woodworth and Pasternack 2022). We acknowledge that this relationship is more complex than a simple link to hydromorphological processes, as it can also be shaped by longitudinal and seasonal requirements as well as individual growth (Rosenfeld et al. 2007; Leunda et al. 2012; Newson et al. 2012; Wolter et al. 2016).

The near-equilibrium sediment supply, through the substantial morphological reworking, increased the shoreline length (i.e., the perimeter of the wetted area) by enhancing the connectivity between the channel and the widening region and, therefore, increased the JBT habitats, a trend that was not observed at the reduced sediment scenarios. For the ABT habitats, the morphological reworking at the near-equilibrium scenarios led to mostly depositions at the main channels and eroding the bank laterally (Rachelly et al. 2022). At low flows, this led the flow to be diverted toward the eroded bank (where habitats were gained) and abandoned the old channel (where habitats were lost) (Figure 8). At higher flows, the deposited sediments at the main channel allowed the flow to access the widening region at average flow conditions (and later after the HQ30 flood at low flow conditions), inundating an inactive morphological region (where habitats were gained). For the reduced sediment scenarios, on the other hand, the limited morphological activities at

these scenarios were restricted to homogenizing the alternating bar morphologies by depositing the thalweg (where the habitats were lost at low flows) and eroding the bars' tops (where the habitats lost at high flows). While this trend provided a minor increase in habitats for ABT at low flow conditions (as the bars' top became accessible at lower flows), this decimated the flow variability provided by the alternating bars and caused habitat reductions at higher flow conditions (Figures A2 and A3). At high flows, the cumulative distribution results shows that habitat gain was associated to deposition (Figure 10), which is largely related to the physical model configuration (Figure 8b). The eroded sediment from the downstream meander deposited at the inner bend, forming a low-lying accessible floodplain featuring favorable conditions for ABT. This further illustrates complexity of linking the fish habitat dynamics with morphodynamic processes, as the driving processes may occur at a spatial extent/scale different from where the preferred features are located (Newson and Newson 2000; Hohensinner et al. 2018; Scott et al. 2022).

Although our results of the ABT habitat dynamics with morphological changes contrast other literatures who reported habitat degradation (i.e., habitat lost) associated with erosional changes and habitat improvement (i.e., habitat gained) associated with depositional changes (Wheaton, Brasington, Darby, and Sear 2010; Moniz and Pasternack 2021; Servanzi et al. 2023), we show that these driving processes can be different in evolving widening restorations. Therefore, erosional or depositional changes are not inherently associated with habitat gain or loss; rather, how these processes modify key hydraulic units (directly or indirectly) determine the effect on habitats and their dynamics. Our results, however, align with Harrison et al. (2011) in suggesting that erosional processes can sometimes be beneficial for habitat replenishment (increased the pool habitats). The relationship between sustained habitat and morphological changes at the reduced supply scenarios showed to be consistent with literature where they associate with minor morphological changes (Wheaton, Brasington, Darby, Merz, et al. 2010; Harrison et al. 2011; Moniz and Pasternack 2021; Servanzi et al. 2023). For the near-equilibrium scenarios, however, the apparent association of the sustained habitats with depositional changes was influenced by the comparison approach, where the HQ30 flood phase was evaluated relative to the initial state (T_2–T_0). In this comparison, sustained habitats were, by definition, restricted to areas that were already suitable in the initial state, which in our case corresponded to the old main channel where deposition dominated. To check whether this pattern reflected the HQ30 flood effect alone, we additionally compared the Widening and After HQ30 states (T_2–T_1). In this additional comparison, sustained habitats were also associated with minor morphological changes (Figure A11), which aligns with the reduced-sediment scenarios results and literature.

Overall, our study aligns with the studies emphasizing how sediment supply is key in sustaining habitat complexity in dynamic river systems, and in promoting fluvial habitats' abundance and dynamics (e.g., Gurnell et al. 2016). River reaches with sediment supply deficiencies, such as dam-impacted reaches, may have restricted habitat complexity and limited morphological activities, making them resistant to be activated by widening restorations or flood events (e.g., Kondolf et al. 2014). As a result, their morphological processes, and therefore their habitat complexity, remain suppressed.

4.4 | Limitations

While our results enhance the understanding of the role of sediment supply in fish habitat dynamics, the generalizability of the results to other river reaches and widening configurations might be limited by our specific settings and choices. The morphological trajectories obtained from the experiment might be constrained by the specificity of the configuration including the one-sided widening, the predefined vertical offset, longitudinal slope, and inlet–outlet alignment, all can potentially influence the direction, rate, and magnitude of widening evolution and morphological behaviors (i.e., near-equilibrium vs. reduced-sediment scenarios) (Demuth et al. 2025). We also noticed that the initial flat widening region might have resulted in an overestimation in habitat areas that was observed after the formation phase when the widening became accessible for the near-equilibrium scenarios (Figure 8e). This effect did not persist after the HQ30 as the widening region got largely reworked. The interpretation of the habitat dynamics might be also sensitive to the fish species and habitat modeling approach, as changes there will likely lead to different quantities and spatial distributions. In this study, habitat suitability was estimated using a hydraulic-only HSI approach based on water depth and velocity, while substrate suitability was excluded because spatial substrate maps were not available. This is an important limitation because sediment supply can also influence bed surface characteristics, with reduced sediment supply promoting bed surface coarsening or homogenization and increased sediment supply often associated with bed surface fining (e.g., Nelson et al. 2009; Surian et al. 2009). This is also relevant for the experimental dataset used here, as Rachelly et al. (2022) reported surface coarsening under reduced-sediment supply conditions. Therefore, the exclusion of substrate suitability means that our hydraulic-only habitat model does not capture the potential effects of sediment supply on spawning habitats, which are particularly relevant for adult brown trout, or possibly on benthic habitat conditions. In addition, the suitability curves used here were literature-based rather than site-specific, which may introduce uncertainty in the estimated habitat response. Further uncertainties arise from the use of uniform roughness in the hydrodynamic simulations and from the upscaling of laboratory morphologies to prototype scale. More broadly, the results should be interpreted as changes in hydraulic habitat suitability for juvenile and adult brown trout, rather than as direct evidence of fish presence, recruitment, population response, or ecological success of the widening.

4.5 | Outlooks

While our study aimed at understanding the sediment-habitat dynamics at steady state discharges, gravel-bed reaches are often also impacted by hydropeaking operations that fluctuate the flow (unsteadiness) within short time scale (Hayes et al. 2023). Vanzo et al. (2016) showed that the hydropeaking impact, such as stranding risk, varies strongly depending on the morphological complexity, which is indirectly related to

the sediment regime. Bätz et al. (2024) further advanced this understanding by quantifying how the morphology and hydropeaking, jointly, govern habitat dislocation and persistence at the patch scale. Directly linking these dynamics to sediment regimes could refine future strategies and policies and promote ecological resilience. In addition, because widenings can act as ecological hotspots or nodes within basin-scale gravel-bed river networks, reach-scale analyses of the hydraulic habitat availability dynamics driven by sediment supply can help identify when restored reaches provide suitable habitats and whether they function as persistent or episodic habitat nodes. This could support larger-scale restoration planning and inform metapopulation models that depend on the temporal availability and connectivity of suitable habitats (Benjankar et al. 2025; Padoan et al. 2025).

5 | Conclusions

This study highlights the role of sediment supply in shaping fish habitat dynamics during river widening processes, using hydraulic habitat suitability for juvenile and adult brown trout as fish habitat proxies. Our results show that the widening morphologies formed with near-equilibrium sediment supply significantly increase habitat availability across broad discharge conditions, promoting resilient river environments with more diverse hydraulic conditions. In contrast, the widening morphologies formed with reduced-sediment supply do not improve habitat for brown trout after widening and moderate flood phases. The spatial habitat dynamics analysis shows that the driving morphodynamic processes are life-stage dependent and relate to the location of the preferred morphological features: juvenile habitat dynamics correspond to shoreline length, as they occupy the channel margins, whereas adult habitat dynamics correspond to elevation changes, as they are located within the channels. We highlight the inherent complexity in linking habitat dynamics with morphodynamic processes, as the driving processes may occur at a different spatial extent than where the habitat patches exist. The results of our study highlight the need to consider sediment supply when designing or evaluating river widening projects.

Acknowledgments

This study was conducted as part of the interdisciplinary research program "Hydraulic Engineering and Ecology," currently in its fifth project phase, "Resilient Rivers: Refugia—Connectivity—Stepping Stones", cofunded by the Swiss Federal Office for the Environment (FOEN), contract 21.0202.PJ/CC00D6EEF. The authors wish to thank Dr. Cristina Rachelly and Dr. Volker Weitbrecht for their valuable contribution of the laboratory dataset. During manuscript preparation, the first author used Open AI «ChatGPT 4.5» only to assist with language refinement and readability. All authors thoroughly reviewed the manuscript and take full responsibility for the content. Open access publishing facilitated by Eidgenossische Technische Hochschule Zurich, as part of the Wiley - Eidgenossische Technische Hochschule Zurich agreement via the Consortium Of Swiss Academic Libraries.

Funding

This work was supported by the Swiss Federal Office of the Environment (FOEN), contract 21.0202.PJ/CC00D6EEF.

Conflicts of Interest

The authors declare no conflicts of interest.

Data Availability Statement

The data that support the findings of this study are available from the corresponding author upon reasonable request.

References

Antonetti, M., L. Hoppler, D. Tonolla, D. Vanzo, M. Schmid, and M. Doering. 2023. "Integrating Two-Dimensional Water Temperature Simulations Into a Fish Habitat Model to Improve Hydro- and Thermopeaking Impact Assessment." *River Research and Applications* 39, no. 3: 501–521. https://doi.org/10.1002/rra.4043.

Aramburú-Paucar, J. M., F. Martínez-Capel, C. A. Puig-Mengual, R. Muñoz-Mas, A. Bertagnoli, and D. Tonina. 2024. "A Large Flood Resets Riverine Morphology, Improves Connectivity and Enhances Habitats of a Regulated River." *Science of the Total Environment* 919: 170717. https://doi.org/10.1016/j.scitotenv.2024.170717.

Bätz, N., C. Judes, D. Vanzo, et al. 2024. "Patch-Scale Habitat Dynamics: Three Metrics to Assess Ecological Impacts of Frequent Hydropeaking." *Journal of Ecohydraulics* 10: 1–29. https://doi.org/10.1080/24705357.2024.2426790.

Benjankar, R., D. Tonina, A. W. Tranmer, S. Paudel, and A. Shrestha. 2025. "The Importance of Floodplain Width on Hydraulic Variability and Aquatic-Riparian Habitat in Semi-Confined, Regulated River Systems." *Ecological Engineering* 216: 107637. https://doi.org/10.1016/j.ecoleng.2025.107637.

Bertoldi, W., M. Welber, L. Mao, S. Zanella, and F. Comiti. 2014. "A Flume Experiment on Wood Storage and Remobilization in Braided River Systems." *Earth Surface Processes and Landforms* 39, no. 6: 804–813. https://doi.org/10.1002/esp.3537.

Boavida, I., V. Dias, M. T. Ferreira, and J. M. Santos. 2014. "Univariate Functions Versus Fuzzy Logic: Implications for Fish Habitat Modeling." *Ecological Engineering* 71: 533–538. https://doi.org/10.1016/j.ecoleng.2014.07.073.

Bolland, J. D., A. D. Nunn, M. C. Lucas, and I. G. Cowx. 2012. "The Importance of Variable Lateral Connectivity Between Artificial Floodplain Waterbodies and River Channels." *River Research and Applications* 28, no. 8: 1189–1199. https://doi.org/10.1002/rra.1498.

Bouloy, A., J.-M. Olivier, J. Riquier, E. Castella, P. Marle, and N. Lamouroux. 2024. "Spatio-Temporal Dynamics of Habitat Use by Fish in a Restored Alluvial Floodplain Over Two Decades." *Science of the Total Environment* 906: 167540. https://doi.org/10.1016/j.scitotenv.2023.167540.

Capra, H., P. Breil, and Y. Souchon. 1995. "A New Tool to Interpret Magnitude and Duration of Fish Habitat Variations." *Regulated Rivers: Research & Management* 10, no. 2–4: 281–289. https://doi.org/10.1002/rrr.3450100221.

Cashman, M. J., G. Lee, L. E. Staub, M. P. Katoski, and K. O. Maloney. 2024. "Physical Habitat Is More Than a Sediment Issue: A Multi-Dimensional Habitat Assessment Indicates New Approaches for River Management." *Journal of Environmental Management* 371: 123139. https://doi.org/10.1016/j.jenvman.2024.123139.

Demuth, P., D. F. Vetsch, R. M. Boes, and V. Weitbrecht. 2025. "Effect of Bank Height on Morphodynamics in a One-Sided Widened Gravel-Bed River." *Earth Surface Processes and Landforms* 50, no. 15: e70183. https://doi.org/10.1002/esp.70183.

Doering, M., R. Freimann, N. Antenen, et al. 2021. "Microbial Communities in Floodplain Ecosystems in Relation to Altered Flow Regimes and Experimental Flooding." *Science of the Total Environment* 788: 147497. https://doi.org/10.1016/j.scitotenv.2021.147497.

Dudgeon, D., A. H. Arthington, M. O. Gessner, et al. 2006. "Freshwater Biodiversity: Importance, Threats, Status and Conservation Challenges." *Biological Reviews of the Cambridge Philosophical Society* 81, no. 2: 163–182. https://doi.org/10.1017/S1464793105006950.

Farò, D., and C. Wolter. 2024. "Integrating Habitat Suitability and Larval Drift Modeling for Spawning-To-Nursery Functional Habitat Connectivity Analysis in Rivers." *Water Resources Research* 60, no. 9: e2023WR036827. https://doi.org/10.1029/2023WR036827.

Gurnell, A. M., D. Corenblit, D. García de Jalón, et al. 2016. "A Conceptual Model of Vegetation-Hydrogeomorphology Interactions Within River Corridors." *River Research and Applications* 32, no. 2: 142–163. https://doi.org/10.1002/rra.2928.

Gurnell, A. M., H. Piégay, F. J. Swanson, and S. V. Gregory. 2002. "Large Wood and Fluvial Processes." *Freshwater Biology* 47, no. 4: 601–619. https://doi.org/10.1046/j.1365-2427.2002.00916.x.

Harrison, L. R., C. J. Legleiter, M. A. Wydzga, and T. Dunne. 2011. "Channel Dynamics and Habitat Development in a Meandering, Gravel Bed River." *Water Resources Research* 47, no. 4: W04513. https://doi.org/10.1029/2009WR008926.

Hauer, C., G. Unfer, P. Holzapfel, M. Haimann, and H. Habersack. 2014. "Impact of Channel Bar Form and Grain Size Variability on Estimated Stranding Risk of Juvenile Brown Trout During Hydropeaking." *Earth Surface Processes and Landforms* 39, no. 12: 1622–1641. https://doi.org/10.1002/esp.3552.

Hauer, C., G. Unfer, S. Schmutz, and H. Habersack. 2008. "Morphodynamic Effects on the Habitat of Juvenile Cyprinids (*Chondrostoma nasus*) in a Restored Austrian Lowland River." *Environmental Management* 42, no. 2: 279–296. https://doi.org/10.1007/s00267-008-9118-2.

Hayes, D. S., J. M. Brändle, C. Seliger, B. Zeiringer, T. Ferreira, and S. Schmutz. 2018. "Advancing Towards Functional Environmental Flows for Temperate Floodplain Rivers." *Science of the Total Environment* 633: 1089–1104. https://doi.org/10.1016/j.scitotenv.2018.03.221.

Hayes, D. S., M. C. Bruno, M. Alp, et al. 2023. "100 Key Questions to Guide Hydropeaking Research and Policy." *Renewable and Sustainable Energy Reviews* 187: 113729. https://doi.org/10.1016/j.rser.2023.113729.

Heggenes, J. 1996. "Habitat Selection by Brown Trout (*Salmo trutta*) and Young Atlantic Salmon (*S. SALAR*) in Streams: Static and Dynamic Hydraulic Modelling." *Regulated Rivers: Research and Management* 12, no. 2–3: 155–169. https://doi.org/10.1002/(sici)1099-1646(199603)12:2/3<155::aid-rrr387>3.0.co;2-d.

Hohensinner, S., C. Hauer, and S. Muhar. 2018. "River Morphology, Channelization, and Habitat Restoration." In *Riverine Ecosystem Management: Science for Governing Towards a Sustainable Future*, edited by S. Schmutz and J. Sendzimir, 41–65. Springer International Publishing. https://doi.org/10.1007/978-3-319-73250-3_3.

Hohensinner, S., M. Jungwirth, S. Muhar, and S. Schmutz. 2011. "Spatio-Temporal Habitat Dynamics in a Changing Danube River Landscape 1812-2006." *River Research and Applications* 27, no. 8: 939–955. https://doi.org/10.1002/rra.1407.

Huet, M. 1949. "Aperçu des relations entre la pente et les populations piscicoles des eaux courantes." *Schweizerische Zeitschrift für Hydrologie* 11, no. 3: 332–351. https://doi.org/10.1007/BF02503356.

Kondolf, G. M. 1997. "PROFILE: Hungry Water: Effects of Dams and Gravel Mining on River Channels." *Environmental Management* 21, no. 4: 533–551. https://doi.org/10.1007/s002679900048.

Kondolf, G. M., Y. Gao, G. W. Annandale, et al. 2014. "Sustainable Sediment Management in Reservoirs and Regulated Rivers: Experiences From Five Continents." *Earth's Future* 2, no. 5: 256–280. https://doi.org/10.1002/2013ef000184.

Lane, S. N., K. S. Richards, and J. H. Chandler. 1996. "Discharge and Sediment Supply Controls on Erosion and Deposition in a Dynamic Alluvial Channel." *Geomorphology* 15, no. 1: 1–15. https://doi.org/10.1016/0169-555X(95)00113-J.

Leunda, P. M., M. Sistiaga, J. Oscoz, and R. Miranda. 2012. "Ichthyofauna of a Near-Natural Pyrenean River: Spatio-Temporal Variability and Reach-Scale Habitat." *Environmental Engineering and Management Journal* 11, no. 6: 1111–1124. https://doi.org/10.30638/eemj.2012.135.

Mandlburger, G., C. Hauer, M. Wieser, and N. Pfeifer. 2015. "Topo-Bathymetric LiDAR for Monitoring River Morphodynamics and Instream Habitats-A Case Study at the Pielach River." *Remote Sensing* 7, no. 5: 6160–6195. https://doi.org/10.3390/rs70506160.

McCabe, C. L., C. D. Matthaei, and J. D. Tonkin. 2025. "The Ecological Benefits of More Room for Rivers." *Nature Water* 3: 260–270. https://doi.org/10.1038/s44221-025-00403-0.

McKean, J., and D. Tonina. 2013. "Bed Stability in Unconfined Gravel Bed Mountain Streams: With Implications for Salmon Spawning Viability in Future Climates." *Journal of Geophysical Research: Earth Surface* 118, no. 3: 1227–1240. https://doi.org/10.1002/jgrf.20092.

Moniz, P. J., and G. B. Pasternack. 2021. "Chinook Salmon Rearing Habitat–Discharge Relationships Change as a Result of Morphodynamic Processes." *River Research and Applications* 37, no. 10: 1386–1399. https://doi.org/10.1002/rra.3855.

Montgomery, D. R., and H. Piégay. 2003. "Wood in Rivers: Interactions With Channel Morphology and Processes." *Geomorphology* 51, no. 1: 1–5. https://doi.org/10.1016/S0169-555X(02)00322-7.

Mortensen, J. G., P. Y. Julien, B. Corsi, C. Radobenko, and T. Anderson. 2024. "Impacts of Hydrologic and Geomorphic Alteration to the Availability of Shallow, Low-Velocity Habitats in an Intensively Managed Arid-Land River." *River Research and Applications* 40: 1808–1824. https://doi.org/10.1002/rra.4338.

Nelson, P. A., J. G. Venditti, W. E. Dietrich, et al. 2009. "Response of Bed Surface Patchiness to Reductions in Sediment Supply." *Journal of Geophysical Research: Earth Surface* 114, no. F2: F02005. https://doi.org/10.1029/2008JF001144.

Newson, M., D. Sear, and C. Soulsby. 2012. "Incorporating Hydromorphology in Strategic Approaches to Managing Flows for Salmonids." *Fisheries Management and Ecology* 19, no. 6: 490–499. https://doi.org/10.1111/j.1365-2400.2011.00822.x.

Newson, M. D., and C. L. Newson. 2000. "Geomorphology, Ecology and River Channel Habitat: Mesoscale Approaches to Basin-Scale Challenges." *Progress in Physical Geography: Earth and Environment* 24, no. 2: 195–217. https://doi.org/10.1177/030913330002400203.

Padoan, F., G. Calvani, G. De Cesare, and P. Perona. 2025. "Hydraulic Drive Framework on Habitat Suitability Enhances Movement Bias of Brown Trout in Stream Networks." *Scientific Reports* 15, no. 1: 16688. https://doi.org/10.1038/s41598-025-00216-x.

Palmer, M. A., H. L. Menninger, and E. Bernhardt. 2010. "River Restoration, Habitat Heterogeneity and Biodiversity: A Failure of Theory or Practice?" *Freshwater Biology* 55, no. SUPPL. 1: 205–222. https://doi.org/10.1111/j.1365-2427.2009.02372.x.

Pauli, M., L. Hunzinger, and O. Hitz. 2018. "More Bed Load in Rivers. Achieving a Sediment Balance Close to the Natural State." *Journal of Applied Water Engineering and Research* 6, no. 4: 274–282. https://doi.org/10.1080/23249676.2018.1497554.

Peipoch, M., M. Brauns, F. R. Hauer, M. Weitere, and H. M. Valett. 2015. "Ecological Simplification: Human Influences on Riverscape Complexity." *Bioscience* 65, no. 11: 1057–1065. https://doi.org/10.1093/biosci/biv120.

Poff, N., J. D. Allan, M. B. Bain, et al. 1997. "The Natural Flow Regime A Paradigm for River Conservation and Restoration." *Bioscience* 47, no. 11: 769–784. https://doi.org/10.2307/1313099.

Rachelly, C. 2021. *Sediment Supply Control on River Widening Morphodynamics and Refugia Availability*. ETH Zürich. https://doi.org/10.3929/ethz-b-000536265.

Rachelly, C., K. L. Mathers, C. Weber, V. Weitbrecht, R. M. Boes, and D. F. Vetsch. 2021. "How Does Sediment Supply Influence Refugia Availability in River Widenings?" *Journal of Ecohydraulics* 6, no. 2: 121–138. https://doi.org/10.1080/24705357.2020.1831415.

Rachelly, C., D. F. Vetsch, R. M. Boes, and V. Weitbrecht. 2022. "Sediment Supply Control on Morphodynamic Processes in Gravel-Bed River Widenings." *Earth Surface Processes and Landforms* 47: 3415–3434. https://doi.org/10.1002/esp.5460.

Reid, D. A., M. A. Hassan, S. Bird, R. Pike, and P. Tschaplinski. 2020. "Does Variable Channel Morphology Lead to Dynamic Salmon Habitat?" *Earth Surface Processes and Landforms* 45, no. 2: 295–311. https://doi.org/10.1002/esp.4726.

Robinson, C. T., U. Uehlinger, and M. T. Monaghan. 2003. "Effects of a Multi-Year Experimental Flood Regime on Macroinvertebrates Downstream of a Reservoir." *Aquatic Sciences* 65, no. 3: 210–222. https://doi.org/10.1007/s00027-003-0663-8.

Rohde, S., M. Schütz, F. Kienast, and P. Englmaier. 2005. "River Widening: An Approach to Restoring Riparian Habitats and Plant Species." *River Research and Applications* 21, no. 10: 1075–1094. https://doi.org/10.1002/rra.870.

Rollet, A. J., H. Piégay, S. Dufour, G. Bornette, and H. Persat. 2014. "Assessment of Consequences of Sediment Deficit on a Gravel River Bed Downstream of Dams in Restoration Perspectives: Application of a Multicriteria, Hierarchical and Spatially Explicit Diagnosis." *River Research and Applications* 30, no. 8: 939–953. https://doi.org/10.1002/rra.2689.

Rosenfeld, J. S., J. Post, G. Robins, and T. Hatfield. 2007. "Hydraulic Geometry as a Physical Template for the River Continuum: Application to Optimal Flows and Longitudinal Trends in Salmonid Habitat." *Canadian Journal of Fisheries and Aquatic Sciences* 64, no. 5: 755–767. https://doi.org/10.1139/F07-020.

Scott, D. N., S. Shahverdian, R. Flitcroft, and E. Wohl. 2022. "Geomorphic Heterogeneity as a Framework for Assessing River Corridor Processes and Characteristics." *River Research and Applications* 38, no. 10: 1893–1901. https://doi.org/10.1002/rra.4036.

Servanzi, L., S. Quadroni, and P. Espa. 2023. "Hydro-Morphological Alteration and Related Effects on Fish Habitat Induced by Sediment Management in a Regulated Alpine River." *International Journal of Sediment Research* 39: 514–530. https://doi.org/10.1016/j.ijsrc.2023.10.001.

Soto Parra, T., E. Politti, and G. Zolezzi. 2024. "Morphological and Fish Mesohabitat Dynamics Following an Experimental Flood Under Different Sediment Availability." *Earth Surface Processes and Landforms* 49: 5167–5185. https://doi.org/10.1002/esp.6025.

Sukhodolov, A., W. Bertoldi, C. Wolter, N. Surian, and M. Tubino. 2009. "Implications of Channel Processes for Juvenile Fish Habitats in Alpine Rivers." *Aquatic Sciences* 71, no. 3: 338–349. https://doi.org/10.1007/s00027-009-9199-x.

Sullivan, S. M. P., and M. C. Watzin. 2009. "Stream-Floodplain Connectivity and Fish Assemblage Diversity in the Champlain Valley, Vermont, U.S.A." *Journal of Fish Biology* 74, no. 7: 1394–1418. https://doi.org/10.1111/j.1095-8649.2009.02205.x.

Surian, N., L. Ziliani, F. Comiti, M. A. Lenzi, and L. Mao. 2009. "Channel Adjustments and Alteration of Sediment Fluxes in Gravel-Bed Rivers of North-Eastern Italy: Potentials and Limitations for Channel Recovery." *River Research and Applications* 25, no. 5: 551–567. https://doi.org/10.1002/rra.1231.

Talbot, C. J., E. M. Bennett, K. Cassell, et al. 2018. "The Impact of Flooding on Aquatic Ecosystem Services." *Biogeochemistry* 141, no. 3: 439–461. https://doi.org/10.1007/s10533-018-0449-7.

Tamminga, A., and B. Eaton. 2018. "Linking Geomorphic Change due to Floods to Spatial Hydraulic Habitat Dynamics." *Ecohydrology* 11, no. 8: e2018. https://doi.org/10.1002/eco.2018.

Tamminga, A., C. Hugenholtz, B. Eaton, and M. Lapointe. 2015. "Hyperspatial Remote Sensing of Channel Reach Morphology and Hydraulic Fish Habitat Using an Unmanned Aerial Vehicle (UAV): A First Assessment in the Context of River Research and Management." *River Research and Applications* 31, no. 3: 379–391. https://doi.org/10.1002/rra.2743.

Tonolla, D., V. Acuña, U. Uehlinger, T. Frank, and K. Tockner. 2010. "Thermal Heterogeneity in River Floodplains." *Ecosystems* 13, no. 5: 727–740. https://doi.org/10.1007/s10021-010-9350-5.

van Rooijen, E., A. Siviglia, D. F. Vetsch, R. M. Boes, and D. Vanzo. 2024. "Quantifying Fluvial Habitat Changes due to Multiple Subsequent Floods in a Braided Alpine Reach." *Journal of Ecohydraulics* 9: 1–21. https://doi.org/10.1080/24705357.2022.2105755.

Vanzo, D., S. Peter, L. Vonwiller, et al. 2021. "BASEMENT v3: A Modular Freeware for River Process Modelling Over Multiple Computational Backends." *Environmental Modelling & Software* 143: 105102. https://doi.org/10.3929/ethz-b-000482308.

Vanzo, D., G. Zolezzi, and A. Siviglia. 2016. "Eco-Hydraulic Modelling of the Interactions Between Hydropeaking and River Morphology." *Ecohydrology* 9, no. 3: 421–437. https://doi.org/10.1002/eco.1647.

Vetsch, D., A. Siviglia, P. Bacigaluppi, et al. 2023. *System Manuals of BASEMENT, Version 4.0.0*. Laboratory of Hydraulics, Glaciology and Hydrology (VAW). ETH Zurich.

Wakeley, J. S. 1988. "A Method to Create Simplified Versions of Existing Habitat Suitability Index (HSI) Models." *Environmental Management* 12, no. 1: 79–83. https://doi.org/10.1007/BF01867379.

Ward, J. V., K. Tockner, and F. Schiemer. 1999. "Biodiversity of Floodplain River Ecosystems: Ecotones and connectivity1." *Regulated Rivers: Research & Management* 15, no. 1–3: 125–139. https://doi.org/10.1002/(sici)1099-1646(199901/06)15:1/3<125::aid-rrr523>3.0.co;2-e.

Wheaton, J. M., J. Brasington, S. E. Darby, et al. 2010. "Linking Geomorphic Changes to Salmonid Habitat at a Scale Relevant to Fish." *River Research and Applications* 26, no. 4: 469–486. https://doi.org/10.1002/rra.1305.

Wheaton, J. M., J. Brasington, S. E. Darby, A. Kasprak, D. Sear, and D. Vericat. 2013. "Morphodynamic Signatures of Braiding Mechanisms as Expressed Through Change in Sediment Storage in a Gravel-Bed River." *Journal of Geophysical Research: Earth Surface* 118, no. 2: 759–779. https://doi.org/10.1002/jgrf.20060.

Wheaton, J. M., J. Brasington, S. E. Darby, and D. A. Sear. 2010. "Accounting for Uncertainty in DEMs From Repeat Topographic Surveys: Improved Sediment Budgets." *Earth Surface Processes and Landforms* 35, no. 2: 136–156. https://doi.org/10.1002/esp.1886.

Wohl, E. 2024. "Resilience in River Corridors: How Much Do we Need?" *Perspectives of Earth and Space Scientists* 5, no. 1: e2023CN000226. https://doi.org/10.1029/2023cn000226.

Wohl, E., B. P. Bledsoe, R. B. Jacobson, et al. 2015. "The Natural Sediment Regime in Rivers: Broadening the Foundation for Ecosystem Management." *Bioscience* 65, no. 4: 358–371. https://doi.org/10.1093/biosci/biv002.

Wohl, E., S. N. Lane, and A. C. Wilcox. 2015. "The Science and Practice of River Restoration." *Water Resources Research* 51, no. 8: 5974–5997. https://doi.org/10.1002/2014WR016874.

Wolter, C., A. D. Buijse, and P. Parasiewicz. 2016. "Temporal and Spatial Patterns of Fish Response to Hydromorphological Processes." *River Research and Applications* 32, no. 2: 190–201. https://doi.org/10.1002/rra.2980.

Woodworth, K. A., and G. B. Pasternack. 2022. "Are Dynamic Fluvial Morphological Unit Assemblages Statistically Stationary Through Floods of Less Than Ten Times Bankfull Discharge?" *Geomorphology* 403: 108135. https://doi.org/10.1016/j.geomorph.2022.108135.

Yarnell, S. M., G. E. Petts, J. C. Schmidt, et al. 2015. "Functional Flows in Modified Riverscapes: Hydrographs, Habitats and Opportunities." *Bioscience* 65, no. 10: 963–972. https://doi.org/10.1093/biosci/biv102.

Supporting Information

Additional supporting information can be found online in the Supporting Information section. **Figure A1:** (a) Discharge time series for the Kandar-Honrich gauging station from 1980 to 2021. (b) Flow duration curve derived from the discharge time-series with key discharge values indicated by horizontal dashed lines. **Figure A2:** Depth percentile vs. discharge for four sediment supply and three morphological states. **Figure A3:** Velocity percentile vs. discharge for four sediment supply and three morphological states. **Figure A4:** Total normalized suitable area variation with discharge at three morphological states (i.e., channelized, widening, and after HQ30) for different sediment supply conditions for juvenile brown trout (JBT) and adult brown trout (ABT). The line represents the habitat area estimated using total habitat suitability index (HSI) of 0.5. The respective filled band represents the habitat area estimated for HSI of 0.25 and 0.75. **Figure A5:** Normalized suitable area duration curve in an average year for 100% and 20% SSL scenarios at different morphological states for (a) juvenile and (b) adult brown trout. The vertical gray dash line indicates the discharge scenario of 4 Q/Q_{m} with corresponding exceedance of 2.4 days per year. **Figure A6:** Relationship between lost habitat and elevation change from the channelized phase at discharges of 0.25, 2.0, and 4.0 Q_m for Juvenile (a to f) and Adult (g to l) Brown Trout. **Figure A7:** Relationship between gained habitat and elevation change from the channelized phase at discharges of 0.25, 2.0, and 4.0 Q_m for Juvenile (a to f) and Adult (g to l) Brown Trout. **Figure A8:** Relationship between sustained habitat and elevation change from the channelized phase at discharges of 0.25, 2.0, and 4.0 Q_m for Juvenile (a to f) and Adult (g to l) Brown Trout. **Figure A9:** Shoreline relationship with discharge for four sediment supply and three morphological states. The horizontal dashed line indicates a shoreline length of 2 km/km, corresponding to a straight flat-bed channel. **Figure A10:** Suitable habitat relationship with suitable habitats for adult brown trout (ABT) at four sediment supply and three morphological states. The vertical dashed line indicates a shoreline length of 2 km/km, corresponding to a straight flat-bed channel. **Figure A11:** Cumulative frequency distribution for sustained habitat and average morphological changes from the channelized to widening phase (a) and at widening to after HQ30 flood phase (b) at 0.25 Q_m for 100 & 20% sediment supply scenarios for Adult Brown Trout habitat. **Data S1:** Supporting Information.